SolarPACES 2023, 29th International Conference on Concentrating Solar Power, Thermal, and Chemical Energy Systems

Receivers and Heat Transfer Media and Transport: Point Focus Systems

https://doi.org/10.52825/solarpaces.v2i.966

Published: 28 Aug. 2024

A Planar-Cavity Receiver Configuration for High-Temperature Solar Thermal Processes

Janna Martinek[1] and Zhiwen Ma[1]

[1]National Renewable Energy Laboratory (NREL), Golden, Colorado, USA

Abstract. Next-generation concentrating solar thermal power (CSP) technologies target a wide spectrum of applications including electricity generation, thermochemical processes, and industrial process heat for broad decarbonization potential. Many of these applications require higher temperatures than those of current commercial nitrate salt systems. Particulate materials are promising candidates for next-generation high-temperature heat transfer and low-cost storage media and can facilitate operation over a wide temperature range. However these materials necessitate novel receiver configurations to accept the high incident flux concentrations that enable high solar-to-thermal receiver efficiency. One option is a novel light-trapping planar cavity receiver configuration in which small cavity-like structures are formed from opaque planar surfaces such that a high incident flux concentration at the cavity aperture is reduced to a wall-absorbed solar flux concentration that is manageable within limited wall-to-particle heat transfer rates. The paper introduces the receiver configuration and provides calculated optical performance for a preliminary 50 MWt receiver design.

Keywords: Concentrating Solar Power, Particle Receiver, Numerical Modeling

1. Introduction

Next generation concentrating solar thermal power (CSP) and novel solar thermochemical systems using concentrating solar thermal energy require high operating temperatures exceeding those of traditional nitrate-salt CSP systems. Particle-based systems are attractive for next-generation CSP applications owing to high-temperature stability of inert silica- or alumina-based particulate materials. Particle CSP and thermal energy storage (TES) eliminate low-temperature freezing concerns that limit molten salt and/or molten metal heat transfer media, and use low-cost stable particulate and containment materials. However, particulate heat transfer media have substantially lower heat transfer rates than liquid media, and thus particle receiver designs require novel configurations to accept the high incident solar flux concentrations necessary for high receiver thermal efficiency at high temperature.

Open-cavity falling particle receivers have many potential advantages including rapid heat transfer rates from direct solar irradiation and elimination of solar flux limitations incurred by opaque containment structures [1,2]. However, these receivers face challenges pertaining to scalability, advection thermal loss, sensitivity to wind conditions, and particle loss through the open aperture. In addition, direct solar flux absorption necessitates particulate materials with high solar absorptivity, and the open aperture is infeasible for chemical processes that require a controlled atmospheric environment. Enclosed receiver configurations can be designed to avoid particle loss, use low-cost naturally-occuring particles with lower solar absorptivity, and have potential for chemical processes; however, these receivers are challenged by high temperatures of the containment structures, thermal stress, diurnal thermal cycle-induced creep-

fatigue damage, and resulting limitations on incident flux concentration and thermal efficiency. Opaque enclosed particle receiver designs with either a dense upflow bubbling fluidized bed contained with an array of finned tubes [3,4], or a dense gas-solid countercurrent fluidized bed contained within a tube or narrow channel [5,6], have recently demonstrated promising particle-to-wall heat transfer coefficients on the order of 1000-1500 W/m^2/K at high temperature. However, similar to molten salt receiver configurations, tubular structures in a traditional receiver configuration are typically subjected to incident flux on only one side. Coupled with the comparatively low heat transfer capability of particles, this can result in high thermal stress and correspondingly low allowable incident flux concentration, large receiver physical size, and low thermal efficiency.

Figure 1a illustrates a previous enclosed particle receiver concept involving arrays of hexagonally-shaped absorbers that use a near-blackbody mechanism to trap sunlight and transfer energy to particles flowing downward over the array of tubes [7,8]. Light penetration into the narrow tubes was found to be challenging in this configuration, leading to high temperatures and temperature non-uniformity on the tube walls. In light of these challenges, the design was adapted to the novel configuration shown in Figure 1b. Figure 1b illustrates a conceptual schematic of a subsection of a receiver configuration that consists of corrugated flat panels, in which vertical cavity structures are formed from arrays of planar surfaces. These flat panel surfaces are positioned such that there is a large angle between each panel surface normal vector and the aperture surface normal vector to effectively spread and absorb incident solar flux on the panel walls [9]. The comparatively open nature of the design in Figure 1b compared to that in Figure 1a facilitates light penetration and solar flux absorption uniformity on highly absorptive surfaces.

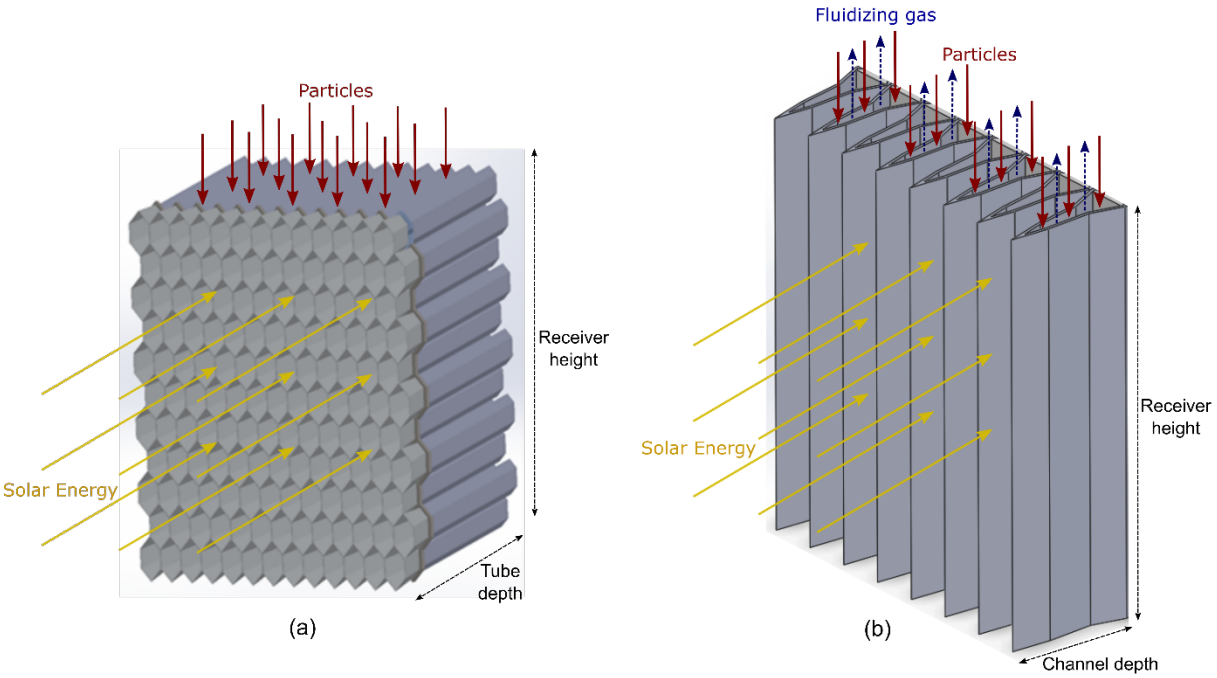

Figure 1. *(a) Previous enclosed particle receiver configuration based on an array of hexagonal tubular absorbers, (b) Sub-section of a novel planar-cavity particle receiver configuration (not to scale)*

This paper introduces the receiver configuration and demonstrates the optical principle of the planar cavities for the design of a receiver involving inert particulate heat transfer media with lower heat transfer capability than a liquid media. Thus, the enclosed nature of the receiver design and overall design principle are also amenable to other gas-phase and thermochemical applications that operate at high temperatures with potentially lower heat transfer coeffiicents.

2. Receiver Configuration and Solar Field Design

The receiver design uses surface orientation to spread incoming solar flux along the receiver panels. In an idealized conceptual scenario, a collimated solar beam (as shown in Figure 1b) incoming normal to the aperture would be distributed along the panel walls by a simple cosine effect. Thus, a high incident solar flux concentration at the cavity aperture can be reduced to a substantially lower absorbed solar flux concentration at the panel walls. The magnitude of the absorbed flux at any given wall in this idealized scenario would be defined simply by the angle of the panel, panel solar absorptivity, and aperture solar flux concentration. A realistic incoming solar beam from a heliostat field will never be ideally collimated; however, careful design of heliostat-to-receiver aiming can predominantly align the specularly-reflected direction for each heliostat with the local aperture normal vector to produce a similar result. Differences in panel absorbed flux between the idealized collimated case and a realistic system result from the distribution of incoming angles arising from sun-shape, optical errors, aiming errors, discrete aimpoint selections, etc. Sets of individual vertical planar cavities such as those shown in Figure 1b can be arranged to form a scalable receiver configuration as shown in Figure 2.

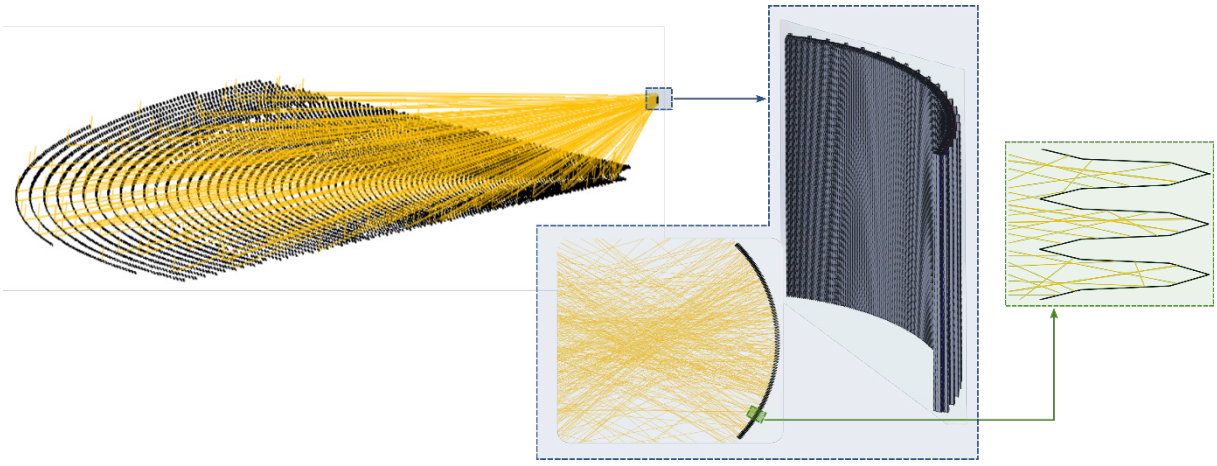

Figure 2. *Example solar field design and 50 MWt receiver configuration*

Receiver panels are constructed of sheet metal using stainless steel or nickel-based alloys such as Haynes 230 or Inconel 740H depending on the receiver working temperature. The solar absorptivity of these sheet metal surfaces can be increased via oxidization or by using a high-temperature surface coating for high solar absorptivity. When oxidized, the absorptivity of nickel alloy panels can reach approximately 90%. Multiple reflections within the cavity configuration trap the sunlight and increase the solar absorption efficiency relative to the solar-weighted absorptivity of the individual surfaces, and thereby achieve high solar absorption efficiency even without absorptive surface coatings. Particles are contained and fluidized within the narrow channels formed between the absorptive panels and flow downward within each channel, achieving the full temperature rise in a single top-to-bottom flow pass. Wall-to-particle heat transfer occurs predominantly by convection/conduction with a small contribution from thermal radiation from the heated walls at high temperature. Correspondingly, the performance is relatively insensitive to the optical properties of the particles, which enables the use of low-cost mined silica sand that is not typically considered for open-cavity directly-irradiated designs due to low solar absorptivity. Furthermore, while only inert applications are considered here, the enclosed natural of the design can facilitate a controlled ambient environment for solar thermochemical processes.

An ideal incident flux distribution for this receiver configuration would: (1) consist of incident beam angles that approximately align with the aperture normal of each cavity to promote solar flux absorption along the full channel depth and a high ratio of aperture incident flux to panel absorbed flux, and (2) provide approximately uniform absorbed power per channel for particle exit temperature uniformity. A north-facing receiver (in the northern hemisphere) is selected to

avoid the typical north/south incident power non-uniformity of an optimized surround heliostat field design, and the particle-containing channels are positioned along the concave arc of a large cylindrical shape. Receiver cavities could be positioned at either the convex front side of the cylinder arc or the concave back side of the cylinder arc; however, the concave curvature can provide additional opportunities to reduce thermal loss.

Solar field designs are created using NREL's SolarPILOT software [10] with heliostat positions restricted to fall within a designated arc angle. Figure 2 illustrates an example of the resulting "wedge-shaped" solar field design and receiver cavities. Image size priority aiming is applied in the height-dimension of the receiver and aimpoints along the receiver circumference are selected to minimize the angle between the heliostat specular reflection and the local aperture surface normal vector.

3. Optical Modeling and Results

Numerous coupled field and receiver design parameters can be tuned to optimize the receiver design and performance, including receiver thermal capacity, heliostat sizing, tower height, receiver height, cylinder diameter, arc angle, and panel configurations (the number of panel sub-sections per channel along with the depth and angle of each sub-section). An integrated modeling tool was developed in Python to facilitate and automate performance evaluation across a wide range of potential design parameters. The tool couples solar field layout (SolarPILOT [10,11]), custom heuristics to adjust heliostat aiming, Monte-Carlo ray tracing to simulate flux profiles (SolTrace [12]), postprocessing, and a reduced-order thermal performance model. While the optical performance is the focus of this paper, Figure 3 illustrates how these optical performance models fit into a full suite of optical, thermal, particle heat transfer, and mechanical models that are currently under development to analyze the receiver configuration.

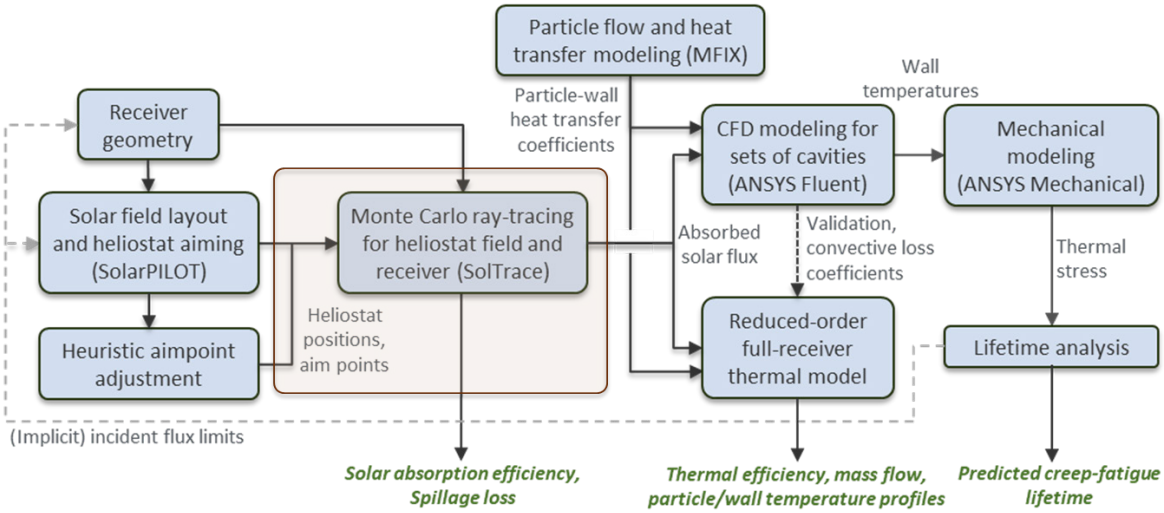

Figure 3. *Solar receiver modeling approach to assess performance and service life. This paper focuses on solar field and flux modeling to demonstrate the basic principles of the planar-cavity design.*

A preliminary base-case 50 MWt field was selected from a sensitivity analysis over receiver height, tower height, and arc angle to balance tradeoffs between field efficiency, spillage loss, projected cost, aperture flux uniformity, and width of the distribution of incoming beam angles at each cavity aperture. Receiver diameter was iteratively adjusted in each case to provide approximately 1000 kW/m^2 peak aperture solar flux concentration at solar noon on the summer solstice. A panel configuration was selected following simulation of various designs selected randomly via Latin Hypercube sampling across six design parameters (panel angle and depth for each of three sections of the particle channel) based on minimizing panel surface area with preliminary approximate constraints on peak absorbed flux at any panel wall and flux uniformity along the cavity depth. Table 1 provides a subset of preliminary base case receiver design

parameters and assumptions used in the analysis. Future analysis will refine this preliminary design based on incident flux constraints informed by panel temperature profiles, thermal stress, and projected service life from the set of models illustrated in Figure 3.

The design parameters in Table 1 produce a nominally 50 MWt receiver configuration with 168 total planar cavity panel modules forming particle flow channels. The solar-weighted absorptivity of the panel walls was assumed to be 90%, consistent with measurements of an oxidized Haynes 230 sample, and all receiver panel surfaces were assumed to reflect diffusely regardless of incidence angle. The solar absorption efficiency was defined to be the ratio of the solar energy absorbed on all panel surfaces to the ratio of the solar energy entering the receiver aperture and, for the base-case parameters in Table 1, was calculated to be 98%. Note that this only captures solar reflection loss and does not include receiver intercept efficiency or thermal loss via convection and IR radiation. Furthermore, protection of the small sharp tip at the front of each module will likely be required, and this is expected to incur additional solar reflection loss. Design options to protect the leading edge are under development, but are not considered in the current study. The ray-tracing model results shown here used 200 to 500 million rays in order to resolve details in the absorbed solar flux profiles on each small panel surface comprising the receiver.

Table 1. *Base case receiver design parameters and simulation assumptions*

Parameter	Value	Parameter	Value
Nominal design point power	50 MWt	Receiver height	6.5 m
Location	Daggett, CA	Receiver diameter	16.4 m
Target peak aperture flux	1000 kW/m^2	Field arc angle	90°
DNI	950 W/m^2	Receiver arc angle	90°
Day	Summer solstice	Number of panel sub-sections	3
Time	Solar noon	Panel 1 angle	10.5°
Sun shape	Limb-darkened	Panel 2 angle	4°
Atmospheric attenuation	DELSOL clear-day	Panel 3 angle	9.5°
Heliostat size	4m x 4m	Panel 1 depth	0.0685 m
Panels per heliostat	1	Panel 2 depth	0.081 m
Heliostat focusing	At slant	Panel 3 depth	0.126 m
Heliostat reflected image error	3 mrad	Panel solar absorptivity	0.9
Tower height	90 m		

Figure 4 illustrates the flux spreading effect on the planar-cavity panel walls. Figure 4a shows the simulated incident flux distribution at the receiver aperture using the inputs in Table 1, where the x-axis represents the position along the curved receiver aperture arc. Figure 4b shows the distributions of absorbed solar flux along the panels comprising the particle channel in the center of the receiver, and Figure 4c shows the distribution along the panels comprising a particle channel near the west edge of the receiver (located at approximately 15% of the total aperture width from the west edge).

The panels in Figure 4b and Figure 4c are arranged from the tip of the channel (left) to the back of the channel (right) with vertical lines denoting the transitions between panel sections. Peak and average incident flux at the curved aperture at the front of the cavities are approximately 967 kW/m^2 and 670 kW/m^2, respectively, while the peak absorbed flux at any receiver surface is only 215 kW/m^2, or approximately 22% of the peak solar flux concentration incident on the receiver aperture. These flux levels are acceptable for particle heat transfer in an enclosed particle receiver to properly control temperatures on the panel walls.

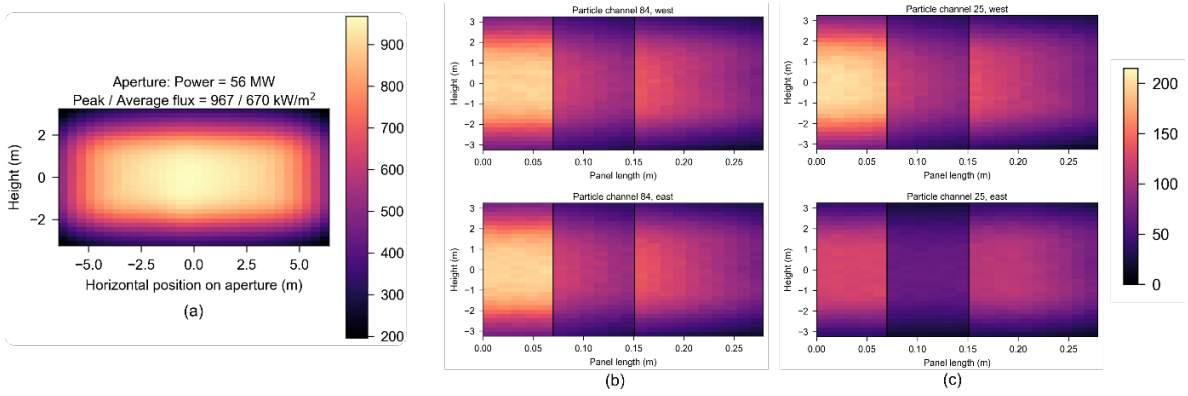

Figure 4. *(a) Incident solar flux distribution on the aperture, (b) Absorbed solar flux distribution along the panels comprising channel 84, (c) Absorbed solar flux distribution along the panels comprising channel 25*

Figure 5 illustrates the peak absorbed solar flux at each panel in the full receiver with 168 planar cavities. The particle flow channel modules are numbered from west to east, and line colors represent the channel wall sub-sections from panel 1 at the tip of the channel (blue, left-most side of the panel flux profiles in Figure 4) to panel 3 at the back of the channel (green, right-most side of the panel flux profiles in Figure 4).

Figure 5 shows that a similar peak absorbed solar flux concentration is maintained over all of the particle channels within the full receiver; however east/west asymmetry in the absorbed flux distributions at the two sides of any given channel (labeled left/right in Figure 5) is observed towards the east/west periphery of the receiver and may have implications on thermal stress and local panel deformation. Figure 5b indicates that the desired solar flux reduction on the panel walls can be maintained at off-design conditions. Note that, for comparison, calculations in Figure 5a and Figure 5b are each presented with an identical DNI rather than the expected clear-sky DNI at the simulated point in time. Actual panel absorbed flux conditions in the morning/afternoon hours would be lower than the values shown here given a lower expected DNI.

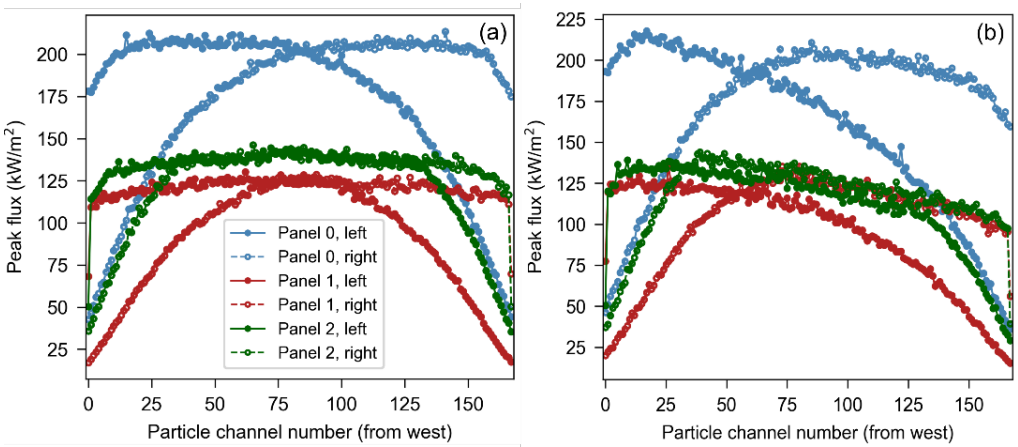

Figure 5. *Peak absorbed solar flux concentration at each panel of the receiver assuming DNI = 950 kW/m² for (a) solar noon on the summer solstice and (b) four hours after solar noon on the summer solstice.*

The simulated flux distributions shown here provide boundary conditions for thermal analysis of the panel modules and subsequent thermal-stress assessment of the panel wall materials (Figure 3).Thermal and mechanical performance are the subjects of ongoing investigations to prove the feasibility of the planar-cavity receiver configuration to support high temperature, high performance operation.

4. Conclusions

This paper introduces a novel enclosed planar cavity receiver configuration designed to support the limited heat transfer capability of a particulate heat transfer medium while maintaining high aperture incident flux concentration necessary for high receiver efficiency. Optical performance simulations for a preliminary 50 MWt receiver design and heliostat field reduced the absorbed flux on the opaque panel walls to approximately 22% of the peak aperture incident flux concentration, with a substantially higher solar absorption efficiency compared to the base solar absorptivity of the wall material. In addition to the optical modeling described here, efforts are underway in experimental testing of fluidization and wall-to-particle heat transfer, particle flow and heat transfer modeling, receiver thermal performance modeling, thermal stress modeling and mechanical analysis, protection strategies for the front tip of the channels, and prototype design and test planning.

Author contributions

Janna Martinek: Conceptualization, Methodology, Analysis, Writing – Original Draft, Visualization **Zhiwen Ma**: Conceptualization, Supervision, Funding Acquisition, Writing – Outline and Draft Revision.

Competing interests

The authors declare no competing interests.

Funding

This material is based upon work supported by the U.S. Department of Energy's Office of Energy Efficiency and Renewable Energy (EERE) under the Solar Energy Technologies Office Award Number 38896.

Acknowledgement

This work was authored by the National Renewable Energy Laboratory, operated by Alliance for Sustainable Energy, LLC, for the U.S. Department of Energy (DOE) under Contract No. DE-AC36-08GO28308. Funding provided by the U.S. Department of Energy Office of Energy Efficiency and Renewable Energy Solar Energy Technologies Office. The views expressed in the article do not necessarily represent the views of the DOE or the U.S. Government. The U.S. Government retains and the publisher, by accepting the article for publication, acknowledges that the U.S. Government retains a nonexclusive, paid-up, irrevocable, worldwide license to publish or reproduce the published form of this work, or allow others to do so, for U.S. Government purposes.

References

1. C. K. Ho, “A review of high-temperature particle receivers for concentrating solar power,” Applied Thermal Engineering, vol. 109 Part B, pp 958-969, Oct. 2016, doi: https://doi.org/10.1016/j.applthermaleng.2016.04.103.
2. B. H. Mills, C. K. Ho, N. R. Schroeder, R. Shaeffer, H. F. Laubscher, K. J. Albrecht, “Design Evaluation of Next-Generation High-Temperature Particle Receiver of Concentrating Solar Thermal Applications”, Energies, vol. 15, pp 1657, Feb. 2022, doi: https://doi.org/10.3390/en15051657.
3. I. Lopez, H. Benoit, D. Gauthier, J-L. Sans, E. Guillot, G. Mazza, G. Flamant "On-sun operation of a 150 kWth pilot solar receiver using dense particle suspension as heat

transfer fluid" Solar Energy, vol. 137, pp 463-476, Nov. 2016, doi: https://doi.org/10.1016/j.solener.2016.08.034.
4. A. Le Gal, B. Grange, M. Tessonneadu, A. Perez, C. Escape, J-L. Sans, G. Flamant, “Thermal analysis of fluidized particle flows in a finned tube solar receiver”, Solar Energy vol. 191, pp 19-33, Oct. 2019, doi: https://doi.org/10.1016/j.solener.2019.08.062.
5. K. Jiang, Y. Kong, C. Xu, Z. Ge, X. Du, “Experimental performance of gas-solid countercurrent fluidized bed particle solar receiver with high-density suspension”, Applied Thermal Engineering, vol. 213, pp 118661, Aug. 2022, doi: https://doi.org/10.1016/j.applthermaleng.2022.118661.
6. D. C. Miller, C. J. Pfutzner, G. S. Jackson, “Heat transfer in counterflow fluidized bed of oxide particles for thermal energy storage”, International Journal of Heat and Mass Transfer, vol. 126 Part B, pp 730-745, Nov 2018, doi: https://doi.org/10.1016/j.ijheatmasstransfer.2018.05.165.
7. A. Fleming, C. Folsom, H. Ban, Z. Ma, “A General Method to Analyze the Thermal Performance of Multi-Cavity Concentrating Solar Power Receivers,” Solar Energy, vol 150, pp 608–618, July 2017, doi: https://doi.org/10.1016/j.solener.2015.08.007
8. J. Martinek, T. Wendelin, Z. Ma, “Predictive Performance Modeling Framework for a Novel Enclosed Particle Receiver Configuration and Application for Thermochemical Energy Storage,” Sol. Energy, vol.166, pp. 409–421, May 2018, doi: https://doi.org/10.1016/j.solener.2018.03.051.
9. Z. Ma, J. Martinek, “Analysis of Solar Receiver Performance for Chemical-Looping Integration with a Concentrating Solar Thermal System”, Journal of Solar Energy Engineering, vol. 141, pp 021003, Apr. 2019, doi: https://doi.org/10.1115/1.4042058.
10. M. J. Wagner, T. Wendelin, “SolarPILOT: A power tower solar field layout and characterization tool”, Solar Energy, vol. 171, June 2018, doi: https://doi.org/10.1016/j.solener.2018.06.063
11. W. T. Hamilton, M. J. Wagner, A. J. Zolan, “Demonstrating SolarPILOT’s Python API Through Heliostat Optimal Aimpoint Strategy Use Case”, Proceedings of ASME 2021 15th International Conference on Energy Sustainability, July 2021, doi: https://doi.org/10.1115/ES2021-60502.
12. T. Wendelin, “SolTRACE: A New Optical Modeling Tool for Concentrating Solar Optics” Proceedings of the ISEC 2003: International Solar Energy Conference, pp. 253-260, Mar. 2003, doi: https://doi.org/10.1115/ISEC2003-44090.